

Exfoliation of Ti_2C and Ti_3C_2 Mxenes from Bulk Phases of Titanium Carbide: A Theoretical Prediction

Krishnakanta Mondal^{†,¶} and Prasenjit Ghosh^{*,‡}

[†]*Department of Physics, Indian Institute of Science Education and Research, Dr. Homi Bhabha Road, Pune-411008, India*

[‡]*Department of Physics, Centre for Energy Sciences, Indian Institute of Science Education and Research, Dr. Homi Bhabha Road, Pune-411008, India*

[¶]*Current affiliation: Department of Physical Sciences, Central University of Punjab, Bathinda, Punjab-151001, India*

E-mail: prasenjit.jnc@gmail.com

Abstract

MXenes, a new class of two dimensional materials with several novel properties, are usually prepared from their MAX phases by etching out the A element using strong chemical reagents. This results in passivation of the surfaces of MXene with different functional groups like O, -OH, -F, etc., which in many cases tend to degrade their properties. In this work, using first principle density functional theory based calculations, we propose a novel method to synthesize pristine Ti_2C and Ti_3C_2 MXenes from the bulk titanium carbides with corresponding stoichiometry. Based on the values of cleavage energy obtained from our calculations, we envisage that pristine Ti_2C and Ti_3C_2 MXenes can be prepared, using mechanical or sonification-assisted liquid-phase exfoliation techniques, from their bulk phases.

Keywords

DFT, 2D Materials, Pristine MXene

Introduction

MXenes, with a general formula of $M_{n+1}X_n$ (M represents a transition metal element, while X can be carbon or nitrogen), are the latest additions to the family of two-dimensional (2D) materials.¹⁻⁶ These newly discovered materials are being extensively investigated due to their novel structural, chemical, optical, and magnetic properties,^{2,3,7-11} which make them promising candidates for various applications such as catalysis, anode materials for Li-ion battery, hydrogen storage, supercapacitors, environmental pollutant decontaminators,^{2,3,7-9} etc. Till date 19 MXenes are experimentally realized and about 50 have been theoretically predicted to be stable.⁶

These MXenes are mainly synthesized from the MAX phase by chemical etching of A-metal, where A is a Group 13 or 14 element.¹² Typically HF, HCl, LiF and NH_4HF are used as etching reagents.^{6,12-16} The surfaces of MXenes prepared from the MAX phases using this method are usually passivated with various chemical groups like -OH, -O, -F, -H etc. Often this surface passivation has degrading effects on the performance of the MXenes. For example, Tang et al., theoretically predicted that the Li ion storage capacity of Ti_3C_2 MXene is larger than that of the -OH or F passivated ones.⁷ Moreover, Junkaew *et al.* reported that the chemical activity of the pristine Ti_2C is higher than that of the O-terminated one.¹⁷ Further, the magnetism of Ti_2C is quenched due the termination of surfaces with O-atom or -OH group.¹⁸ Additionally, due to the unavailability of the pristine MXenes, the experimental researchers are not able to verify several of the theoretically predicted superior properties of MXenes. Therefore, it is highly desirable to develop novel methods, that do not use etching agents, for synthesis of high quality pristine MXenes.

In view of preparing pristine MXene, in 2015, a bottom up approach, with chemical

vapour deposition (CVD) method, was used to synthesize 2D layers of α -Mo₂C.⁵ Using this method a ultrathin (few nano meter) layer of α -Mo₂C was prepared. Similar method was also used to synthesize ultrathin layers of tungsten and tantalum carbides.¹⁹ However, the synthesis of a monolayer of MXene is yet to be demonstrated.⁶ A method leading to the realization of pristine MXene will be a breakthrough in this field. To this end, in this work, using first principles density functional theory (DFT) based calculations, we have proposed a novel process that uses physical methods to synthesize Ti₂C and Ti₃C₂ MXenes from their corresponding titanium carbide bulk phases *without* using etching agents.

Computational details

All the calculations were performed with the Quantum ESPRESSO (QE) package^{20,21} which is an implementation of DFT in a plane wave pseudopotential framework. The electron-electron exchange and correlation functional was described with the Perdew-Burke-Ernzerhof (PBE)²² parametrization of the generalized gradient approximation(GGA). To include the van der Waals correction we have used Grimme’s dispersion method as implemented in QE.²³ The calculations were performed employing kinetic energy cutoffs of 55 and 480 Ry for the wave function and augmentation charge density, respectively. To speed up the convergence, we have used the Marzari-Vanderbilt smearing with a smearing width of 0.007 Ry.²⁴ We have modelled the surfaces of Ti₂C and Ti₃C₂ using six and four layered slabs respectively. Further, to avoid the interactions between the periodic images we have used a vacuum of more than 16 Å along z-axis. We have ensured that this vacuum is maintained even for the case where we have displaced the top most layer to a distance of 10 Å from the layer below it to mimic the exfoliation process. The Brillouin zone has been sampled using 12× 12 × 1 k-points for the slab calculation.

To analyse the interlayer interaction in the bulk phases of Ti₂C and Ti₃C₂ we have carried out NCI (Non Covalent Interaction)^{25,26} analysis, as implemented in CRITIC2 code,^{27,28} on

these systems. NCI analysis is based on the electron density, ρ and its reduced density gradient, s , which is defined in the following,

$$s = \frac{1}{2(3\pi^2)^{1/3}} \frac{|\nabla\rho|}{\rho^{4/3}} \quad (1)$$

The isosurface of s in 3D have been visualised using VMD. The isosurface is colored (blue-green-red color scale) according to the value of $\text{sign}(\lambda_2)\rho$. Blue indicates the weak attractive interaction and green represents the van der Waals interaction while red shows non-bonding interaction.

The formation energy (E_{form}) of the bulk phases of Ti_2C has been calculated using the following equation:

$$E_{form} = \frac{E(\text{Ti}_m\text{C}_n) - m \times \mu(\text{Ti}_{hcp}) - n \times \mu(\text{C}_{grap})}{n + m} \quad (2)$$

where $E(\text{Ti}_m\text{C}_n)$ is the energy of the bulk unitcell of Ti_2C and $\mu(\text{Ti}_{hcp})$ and $\mu(\text{C}_{grap})$ are the chemical potentials of Ti and C atoms, respectively. $\mu(\text{Ti}_{hcp})$ has been calculated from the bulk HCP phase of Ti and $\mu(\text{C}_{grap})$ is taken from the graphite phase of C. m and n indicate the number of Ti and C atoms in the bulk phase of Ti_2C , respectively.

Results and Discussion

We begin by noting that amongst the many polytypes of bulk Ti_2C , the two most stable ones are the trigonal (Figure 1(a)) and the cubic (Figure S1(a)) phases.²⁹⁻³³ Depending on the experimental conditions, both these phases have been successfully synthesized.^{29,31,33} From our calculations we find that, in agreement with previous literature report,³⁰ the cubic phase is about 0.02 eV/atom more stable than the trigonal phase (Table S1). While the cubic phase of Ti_2C have a sodium chloride structure with the C atoms or vacancy surrounded by the distorted octahedra of Ti atoms, the trigonal phase forms a layered structure of the form

Ti-C-Ti, where the Ti atoms in the two hexagonal planes are separated by a plane of C atoms. We note that each Ti-C-Ti layer of the bulk trigonal phase is similar to that of a layer of Ti_2C MXene (Figure 1(c)). Moreover, the in plane lattice parameter of 3.08 \AA of the trigonal phase is also similar to that of the Ti_2C MXene lattice parameter of 3.01 \AA .³⁴

Analogous to the layered trigonal structure of bulk Ti_2C , bulk Ti_3C_2 also have a layered structure with hexagonal symmetry, the layers being stacked along the (0001) direction (Figure 1(b)). Each layer in the bulk hexagonal phase of Ti_3C_2 is constructed with the atomic arrangement of Ti-C-Ti-C-Ti, where the C atoms are sandwiched between Ti layers. It is observed that the in plane lattice parameters (3.07 \AA) of the hexagonal phase of Ti_3C_2 is similar to those of the corresponding MXene (3.10 \AA).¹⁰ Therefore, each layer of Ti-C-Ti-C-Ti in the bulk hexagonal phase of Ti_3C_2 can be identified as the well known Ti_3C_2 MXene.

The above observations of the exceptional similarity between the layered structures of the trigonal (hexagonal) phase of bulk Ti_2C (Ti_3C_2) with that of Ti_2C (Ti_3C_2) MXene stimulated us to ask the question: Is it possible to mechanically exfoliate a single layer of Ti_2C (Ti_3C_2) from the bulk trigonal (hexagonal) phase? If this can be achieved, then it will provide a novel route to synthesize highly desirable pristine Ti_2C and Ti_3C_2 MXenes.

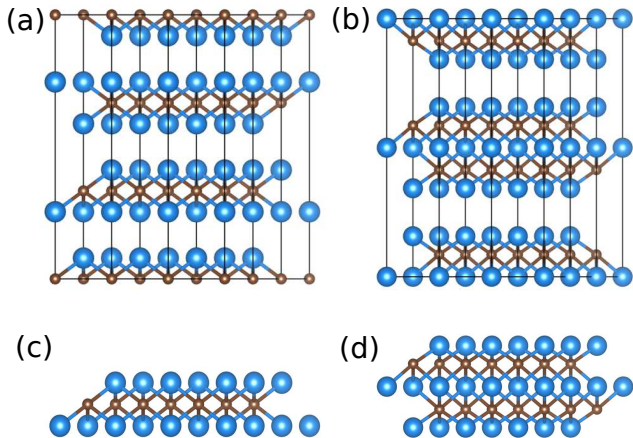


Figure 1: Side view of the structure of bulk phase and MXene of Ti_2C (a, c) and Ti_3C_2 (b, d). In this and the subsequent figures in this manuscript the Ti and C atoms are represented by large blue spheres and small brown spheres, respectively.

To provide an answer to the above mentioned question it is imperative to understand the nature and strength of the interaction between two MXene layers in the bulk phases of Ti_2C and Ti_3C_2 . The charge density distribution between two such layers in the bulk trigonal (hexagonal) phase will provide an indication of the nature and strength of interactions between them. A strong covalent interaction between two layers will result in significant accumulation of charge density between them while weak metallic/van der Waals interaction will result in negligible charge density between two such layers. Figure 2(a) (Figure 2(c)) shows the charge density isosurface plot for the layered bulk phase of Ti_2C (Ti_3C_2). To quantify the interlayer charge density further, we have also plotted in Figure 2(b) (Figure 2(d)) the planar average (averaged over the xy -plane) of the charge density as a function of z along the (0001) direction in bulk Ti_2C (Ti_3C_2). From Figure 2 we find that for both Ti_2C and Ti_3C_2 the charge is localized within the layer with negligible charge density in between the two layers. Further for comparison with Ti_2C (Ti_3C_2) MXene, we have also plotted the planar average of the charge density of MXene in Figure 2(b) (Figure 2(d)). We find that the two charge density profiles are almost identical.

Furthermore, to get more insight into the bonding between the layers we have carried out NCI (Non Covalent Interaction)^{25,26} analysis on the bulk phase of Ti_2C (Ti_3C_2). Figure 3(a) and (b) show the s vs. $\text{sign}(\lambda_2)\rho$ for Ti_2C and Ti_3C_2 respectively. We find that there are tails of s at very low negative values of $\text{sign}(\lambda_2)\rho$ suggesting that there might be weak attractive interactions between the layers. Further we plotted the isosurface of s for $s = 0.1$ (denoted by the blue horizontal line in Figure 3(a) and (b)) for $\text{sign}(\lambda_2)\rho$ between -0.05 and 0.05 a.u. These isosurfaces are shown in Figure 3(c) and (d). The plots show greenish isosurfaces at the interlayer positions thereby further supporting our claim that the interaction between two such layers are indeed weak and of non-covalent origin.

From the above discussion it is clear that the interlayer interaction in bulk Ti_2C (Ti_3C_2) is significantly weak which suggest that a single layer can be exfoliated from a slab of Ti_2C (Ti_3C_2).

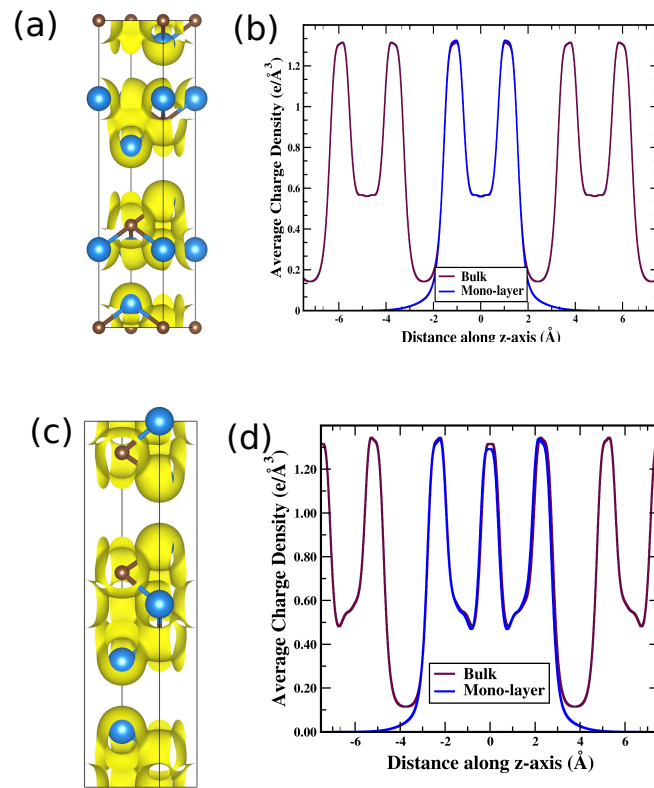


Figure 2: Charge density isosurfaces of the bulk (a) Ti_2C , and (c) Ti_3C_2 . Planar average of charge density of MXene (b) Ti_2C , and (d) Ti_3C_2 .

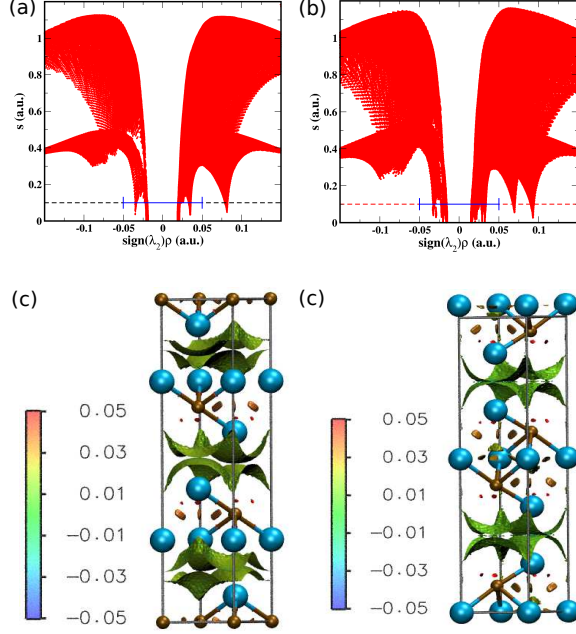


Figure 3: NCI plots for the bulk phases of (a,c) Ti_2C and (b,d) Ti_3C_2 . NCI plots have been shown for $s=0.1$ a.u. (dotted line in (a) and (b)). The color scale shows the range of $\text{sign}(\lambda_2)\rho$ between -0.05 and 0.05 a.u.

Since we have ascertained that the interlayer interactions in bulk trigonal Ti_2C and hexagonal Ti_3C_2 is weak, we proceed to compute the energy cost of exfoliating a single layer of Ti-C-Ti or Ti-C-Ti-C-Ti from their corresponding bulk phases. First, we have investigated the exfoliation of Ti-C-Ti layer from the trigonal phase of Ti_2C . For this purpose we have chosen the (0001) surface of the bulk phase, which is represented by a slab with a thickness of six layers (Slab6) (see Figure S3). From this slab, we gradually exfoliate the surface Ti-C-Ti layer by slowly increasing interlayer distance between the surface Ti-C-Ti layer and that below it. At each step we have performed a constrained relaxation keeping the z-coordinate of the C-atom of the exfoliated surface layer and the middle C-atom of the slab fixed. This step-wise detachment of the surface layer is done till the exfoliated layer does not interact with the rest of the slab. The cleavage energy (E_{cl}) has been calculated using the following equation:

$$E_{cl} = \frac{1}{2A} [E(\text{slab6}) - E^d(\text{slab6})] \quad (3)$$

where $E(\text{slab6})$ is the energy of the Slab6 and $E^d(\text{slab6})$ indicates the energy corresponding

to the Slab6 when the topmost layer is shifted to a distance d away from the Slab6. E_{cl} as a function of d is plotted in Figure 4. A denotes the area of the surface unit cell. We find that the cleavage energy for the single layer is 1.82 J/m^2 . Moreover, to check whether it is easier to cleave a single Ti-C-Ti layer or two such layers during exfoliation, we have also computed the cleavage energy for the exfoliation of bilayer of Ti_2C MXene. For the bilayer, we determine E_{cl} to be 1.78 J/m^2 which is slightly less than that of the single layer. This suggests that during the exfoliation process both bilayers and monolayers will be present. We note that from two such bilayers, single layers can also be exfoliated.

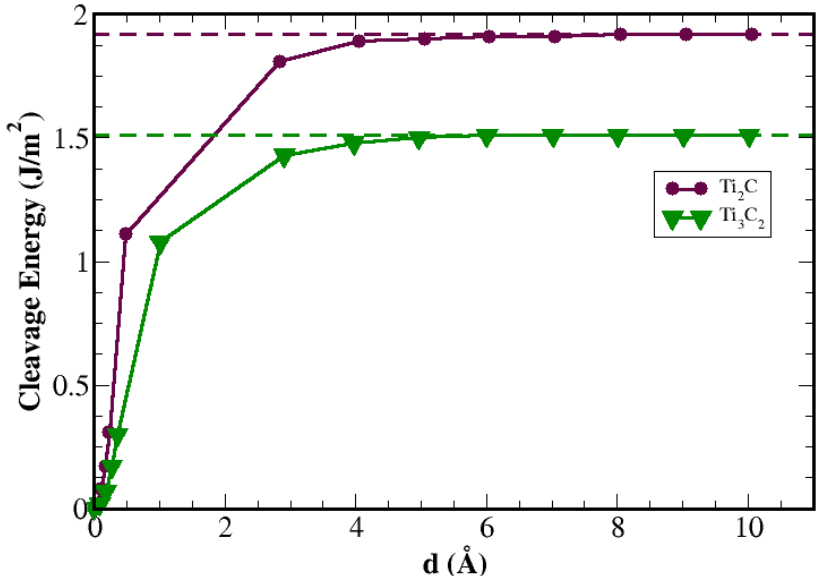


Figure 4: Cleavage energy of the MXenes as a function of the distance (d) of the cleaved layer from the surface.

Following similar exfoliation process described above we have calculated the cleavage energy for the exfoliation of Ti_3C_2 layer from its bulk hexagonal phase. In Figure 4 we have plotted E_{cl} vs d for the case of Ti_3C_2 . The details of the exfoliation process used in the calculations have been described in the Supporting Information. We found the cleavage energy for the exfoliation of Ti_3C_2 to be 1.51 J/m^2 , which is 0.31 J/m^2 lower than the corresponding value for the case of Ti_2C . This indicates that the exfoliation of Ti_3C_2 MXene

from its bulk phase is easier than that for the case of Ti_2C MXene.

In order to provide a perspective as to how easy or difficult to exfoliate a single layer of Ti_2C or Ti_3C_2 , we compare our computed cleavage energy with those reported for other layered materials in literature. For example for exfoliating a single atomic layer thick graphene sheet from bulk graphite the cleavage energy is about 0.37 J/m^2 .³⁵ This tells us that it is about 4-5 times easier to exfoliate graphene from graphite compared to our systems. In contrast, for exfoliating quasi-two dimensional (more than one atomic layer thick) sheets, for example GeP_3 layer from its bulk, the cleavage energy is 1.14 J/m^2 , which is about 0.68 J/m^2 (0.37 J/m^2) higher than that we have observed for Ti_2C (Ti_3C_2). Although the cleavage energy for exfoliating Ti_2C (Ti_3C_2) is larger than those observed for exfoliation of 2D layers from different van der Waals solids, we would like to mention that very recently layered 2D materials have been exfoliated from non-van der Waals solids also. For example, Balan *et al.* have synthesized a novel 2D material “hematene” from natural iron-ore hematite ($\alpha\text{-Fe}_2\text{O}_3$) using liquid exfoliation technique.³⁶ Using a sonification-assisted liquid-phase exfoliation method Yadav *et al.* demonstrated that it is possible to synthesize magnetic 2D material “chromiteen” from naturally occurring mineral chromite (FeCr_2O_4).³⁷ For both these cases, the exfoliation results in cleavage of strong covalent bonds. This suggests that using similar experimental techniques, it is possible to exfoliate Ti_2C and Ti_3C_2 MXenes from their corresponding layered bulk phases. We note that in this case the exfoliation would involve breaking of weaker metallic bonds between the Ti atoms of two interacting Ti-C-Ti or Ti-C-Ti-C-Ti layers depending on the systems.

Conclusions

In summary, we have proposed a novel method to synthesize pristine Ti_2C and Ti_3C_2 MXenes by exfoliation of, respectively, Ti-C-Ti and Ti-C-Ti-C-Ti layers from their corresponding layered bulk phases. Based on our computed cleavage energy and some recent experimental

reports on synthesis of layered magnetic 2D materials from non-van der Waals solids using sonification-assisted liquid-phase exfoliation method, we suggest that use of similar methods in this case will enable experimentalists to exfoliate highly desired pristine Ti_2C and Ti_3C_2 MXenes. We hope that our results will motivate experimentalists to use our proposed methodology to try synthesizing pristine Ti_2C and Ti_3C_2 MXenes.

Acknowledgments

PG would like to acknowledge Dr. Nirmalya Ballav, IISER Pune for helpful discussions. KM and PG would like to acknowledge Department of Science and Technology, India Grant No: EMR/2016/005275 for funding. PG would like to acknowledge Department of Science and Technology-Nanomission, India Grants No: SR/NM/NS-15/2011, SR/NM/NS-1285/2014 and SR/NM/TP-13/2016 for funding.

References

1. Naguib, M.; Kurtoglu, M.; Presser, V.; Lu, J.; Niu, J.; Heon, M.; Hultman, L.; Gogotsi, Y.; Barsoum, M. W. Two-Dimensional Nanocrystals Produced by Exfoliation of Ti_3AlC_2 . *Advanced Materials* **2011**, *23*, 4248–4253.
2. Naguib, M.; Halim, J.; Lu, J.; Cook, K. M.; Hultman, L.; Gogotsi, Y.; Barsoum, M. W. New Two-Dimensional Niobium and Vanadium Carbides as Promising Materials for Li-Ion Batteries. *J. Am. Chem. Soc.* **2013**, *135*, 15966–15969.
3. Naguib, M.; Come, J.; Dyatkin, B.; Presser, V.; Taberna, P.-L.; Simon, P.; Barsoum, M. W.; Gogotsi, Y. MXene: a promising transition metal carbide anode for lithium-ion batteries. *Electrochemistry Communications* **2012**, *16*, 61–64.
4. Khazaei, M.; Arai, M.; Sasaki, T.; Chung, C.-Y.; Venkataramanan, N. S.; Estili, M.; Sakka, Y.; Kawazoe, Y. Novel Electronic and Magnetic Properties of Two-Dimensional

- Transition Metal Carbides and Nitrides. *Advanced Functional Materials* **2013**, *23*, 2185–2192.
- Gogotsi, Y. Chemical vapour deposition: Transition metal carbides go 2D. *Nature Materials* **2015**, *14*, 1079–1080.
 - Anasori, B.; Lukatskaya, M. R.; Gogotsi, Y. 2D metal carbides and nitrides (MXenes) for energy storage. *Nature Reviews Materials* **2017**, *2*, 16098.
 - Tang, Q.; Zhou, Z.; Shen, P. Are MXenes Promising Anode Materials for Li Ion Batteries? Computational Studies on Electronic Properties and Li Storage Capability of Ti₃C₂ and Ti₃C₂X₂ (X = F, OH) Monolayer. *J. Am. Chem. Soc.* **2012**, *134*, 16909–16916.
 - Xie, Y.; Naguib, M.; Mochalin, V. N.; Barsoum, M. W.; Gogotsi, Y.; Yu, X.; Nam, K.-W.; Yang, X.-Q.; Kolesnikov, A. I.; Kent, P. R. C. Role of Surface Structure on Li-Ion Energy Storage Capacity of Two-Dimensional Transition-Metal Carbides. *J. Am. Chem. Soc.* **2014**, *136*, 6385–6394.
 - Lukatskaya, M. R.; Mashtalir, O.; Ren, C. E.; DallAgnese, Y.; Rozier, P.; Taberna, P. L.; Naguib, M.; Simon, P.; Barsoum, M. W.; Gogotsi, Y. Cation Intercalation and High Volumetric Capacitance of Two-Dimensional Titanium Carbide. *Science* **2013**, *341*, 1502–1505.
 - Bai, Y.; Zhou, K.; Srikanth, N.; Pang, J. H. L.; He, X.; Wang, R. Dependence of elastic and optical properties on surface terminated groups in two-dimensional MXene monolayers: a first-principles study. *RSC Adv.* **2016**, *6*, 35731–35739.
 - Guo, Z.; Zhou, J.; Zhu, L.; Sun, Z. MXene: a promising photocatalyst for water splitting. *J. Mater. Chem. A* **2016**, *4*, 11446–11452.
 - Naguib, M.; Mochalin, V. N.; Barsoum, M. W.; Gogotsi, Y. 25th Anniversary Article:

- MXenes: A New Family of Two-Dimensional Materials. *Advanced Materials* **2014**, *26*, 992–1005.
13. Ghidui, M.; Lukatskaya, M. R.; Zhao, M.-Q.; Gogotsi, Y.; Barsoum, M. W. Conductive two-dimensional titanium carbide clay with high volumetric capacitance. *Nature* **2014**, *516*, 78–81.
 14. Wang, L.; Zhang, H.; Wang, B.; Shen, C.; Zhang, C.; Hu, Q.; Zhou, A.; Liu, B. Synthesis and electrochemical performance of Ti₃C₂T_x with hydrothermal process. *Electronic Materials Letters* **2016**, *12*, 702–710.
 15. Halim, J.; Lukatskaya, M. R.; Cook, K. M.; Lu, J.; Smith, C. R.; Nslund, L.-A.; May, S. J.; Hultman, L.; Gogotsi, Y.; Eklund, P. *et al.* Transparent Conductive Two-Dimensional Titanium Carbide Epitaxial Thin Films. *Chem Mater* **2014**, *26*, 2374–2381.
 16. Karlsson, L. H.; Birch, J.; Halim, J.; Barsoum, M. W.; Persson, P. O. A. Atomically Resolved Structural and Chemical Investigation of Single MXene Sheets. *Nano Lett.* **2015**, *15*, 4955–4960.
 17. Junkaew, A.; Arryave, R. Enhancement of the selectivity of MXenes (M₂C, M = Ti, V, Nb, Mo) *via* oxygen-functionalization: promising materials for gas-sensing and -separation. *Physical Chemistry Chemical Physics* **2018**, *20*, 6073–6082.
 18. Xie, Y.; Kent, P. R. C. Hybrid density functional study of structural and electronic properties of functionalized Ti_{*n*+1}X_{*n*} (X = C, N) monolayers. *Phys. Rev. B* **2013**, *87*, 235441.
 19. Xu, C.; Wang, L.; Liu, Z.; Chen, L.; Guo, J.; Kang, N.; Ma, X.-L.; Cheng, H.-M.; Ren, W. Large-area high-quality 2D ultrathin Mo₂C superconducting crystals. *Nature Materials* **2015**, *14*, 1135–1141.

20. Giannozzi, P.; Baroni, S.; Bonini, N.; Calandra, M.; Car, R.; Cavazzoni, C.; Ceresoli, D.; Chiarotti, G. L.; Cococcioni, M.; Dabo, I. *et al.* QUANTUM ESPRESSO: a modular and open-source software project for quantum simulations of materials. *Journal of Physics: Condensed Matter* **2009**, *21*, 395502.
21. Giannozzi, P.; Andreussi, O.; Brumme, T.; Bunau, O.; Nardelli, M. B.; Calandra, M.; Car, R.; Cavazzoni, C.; Ceresoli, D.; Cococcioni, M. *et al.* Advanced capabilities for materials modelling with QUANTUM ESPRESSO. *Journal of Physics: Condensed Matter* **2017**, *29*, 465901.
22. Perdew, J. P.; Burke, K.; Ernzerhof, M. Generalized Gradient Approximation Made Simple. *Phys. Rev. Lett.* **1996**, *77*, 3865.
23. Grimme, S. Semiempirical GGA-type density functional constructed with a long-range dispersion correction. *J. Comput. Chem.* *27*, 1787–1799.
24. Marzari, N.; Vanderbilt, D.; De Vita, A.; Payne, M. C. Thermal Contraction and Disordering of the Al(110) Surface. *Phys. Rev. Lett.* **1999**, *82*, 3296–3299.
25. Johnson, E. R.; Keinan, S.; Mori-Snchez, P.; Contreras-Garcia, J.; Cohen, A. J.; Yang, W. Revealing Noncovalent Interactions. *J. Am. Chem. Soc.* **2010**, *132*, 6498–6506, PMID: 20394428.
26. Contreras-Garcia, J.; Johnson, E. R.; Keinan, S.; Chaudret, R.; Piquemal, J.-P.; Beratan, D. N.; Yang, W. NCIPLLOT: A Program for Plotting Noncovalent Interaction Regions. *J. Chem. Theory and Comput.* **2011**, *7*, 625–632, PMID: 21516178.
27. de-la Roza, A. O.; Johnson, E. R.; Luaa, V. Critic2: A program for real-space analysis of quantum chemical interactions in solids. *Comput. Phys. Commun.* **2014**, *185*, 1007 – 1018.

28. Otero-de-la Roza, A.; Johnson, E. R.; Contreras-Garcia, J. Revealing non-covalent interactions in solids: NCI plots revisited. *Phys. Chem. Chem. Phys.* **2012**, *14*, 12165–12172.
29. Em, V. T.; Tashmetov, M. Y. The Structure of the Ordered Phase in Rocksalt Type Titanium Carbide, Carbidenitride, and Carbidehydride. *physica status solidi (b)* **1996**, *198*, 571–575.
30. Eibler, R. New aspects of the energetics of ordered Ti₂C and Ti₂N. *J. Phys.: Condens. Matter* **2007**, *19*, 196226.
31. Frisk, K. A revised thermodynamic description of the TiC system. *Calphad* **2013**, *27*, 367–373.
32. Hugosson, H. W.; Korzhavyi, P.; Jansson, U.; Johansson, B.; Eriksson, O. Phase stabilities and structural relaxations in substoichiometric TiC_{1-x}. *Phys. Rev. B* **2001**, *63*, 165116.
33. Tashmetov, M. Y.; Em, V. T.; Lee, C. H.; Shim, H. S.; Choi, Y. N.; Lee, J. S. Neutron diffraction study of the ordered structures of nonstoichiometric titanium carbide. *Physica B: Condensed Matter* **2002**, *311*, 318–325.
34. Kurtoglu, M.; Naguib, M.; Gogotsi, Y.; Barsoum, M. W. First principles study of two-dimensional early transition metal carbides. *MRS Communications* **2012**, *2*, 133–137.
35. Jing, Y.; Ma, Y.; Li, Y.; Heine, T. GeP₃: A Small Indirect Band Gap 2D Crystal with High Carrier Mobility and Strong Interlayer Quantum Confinement. *Nano Lett.* **2017**, *17*, 1833–1838.
36. Puthirath Balan, A.; Radhakrishnan, S.; Woellner, C. F.; Sinha, S. K.; Deng, L.; Reyes, C. d. l.; Rao, B. M.; Paulose, M.; Neupane, R.; Apte, A. *et al.* Exfoliation of a non-van der Waals material from iron ore hematite. *Nature Nanotechnology* **2018**, *13*, 602–609.

37. Yadav, T. P.; Shirodkar, S. N.; Lertcumfu, N.; Radhakrishnan, S.; Sayed, F. N.; Malviya, K. D.; Costin, G.; Vajtai, R.; Yakobson, B. I.; Tiwary, C. S. *et al.* Chromiteen: A New 2D Oxide Magnetic Material from Natural Ore. *Adv. Mat. Inter.* **2018**, *5*, 1800549.

Supplementary of Exfoliation of Ti_2C and Ti_3C_2 Mxenes from Bulk Phases of Titanium Carbide: A Theoretical Prediction

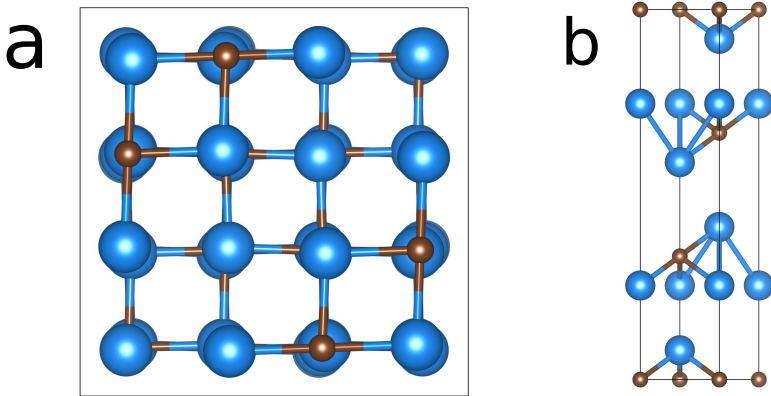


Figure S1: Different stable phases of bulk Ti_2C , (a) Cubic, and (b) Trigonal

Table 1: Comparison of our computed results with those of the reported values.³⁰⁻³² The values within the parenthesis indicate the experimental data taken from ref.³¹ The results obtained with the van der Waals correction are given within the square brackets.

	Cubic		Trigonal	
	our results	reported	our results	reported
E_{form}	-0.66 [-0.71]	-0.68 [-0.70]	-0.64	-
$a(\text{\AA})$	8.64 [8.62]	8.64 (8.60)	3.08 [3.09]	3.09 (3.06)
$c(\text{\AA})$	-	-	14.45 [14.48]	14.45 (14.91)

Slab Convergence Test

It is found that the five layers of Ti_2C , which we named as Slab5, is required to achieve the convergence of the thickness of the slab along (0001). In Figure S2 we have plotted the density of the states (DOS) of the middle layer of this slab along with that of the bulk. From the Figure S2(a) it can be observed that the density of the bulk closely matches with that of the middle layer in slab5. This clearly indicates that the Slab5 can mimic a piece of bulk

Ti₂C. For the case of Ti₃C₂, it is found that the three layers of Ti₃C₂, which we named as

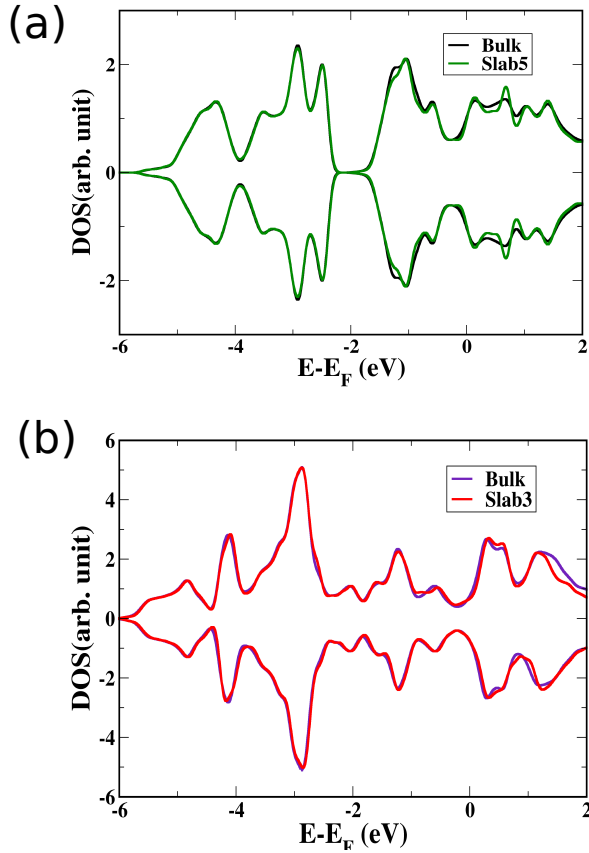


Figure S2: Density of states of (a) Ti₂C and (b) Ti₃C₂.

Slab3, is required to achieve the convergence of the thickness of the slab along (0001). In Figure S2(b) we have plotted the density of the states (DOS) of the middle layer of this slab along with that of the bulk. From the Figure S2 (b) it can be observed that the density of the bulk closely matches with that of the middle layer in slab3. This clearly indicates that the Slab3 can mimic a piece of bulk Ti₃C₂.

Exfoliation of Ti₃C₂ MXene

We have investigated the exfoliation of Ti-C-Ti-C-Ti layer from the trigonal phase of Ti₃C₂. For this purpose we have chosen the (0001) surface of the bulk phase, which is represented by a slab with a thickness of 4 layers (Slab4) (see Figure S3). From this slab, we gradually

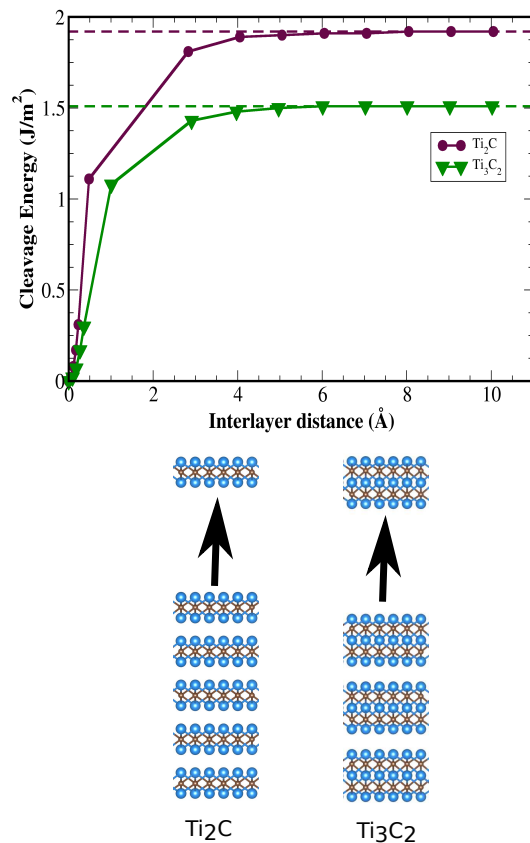


Figure S3: Exfoliation of Ti_2C and Ti_3C_2 .

exfoliate the surface Ti-C-Ti-C-Ti layer. This is done by slowly increasing interlayer distance between the surface Ti-C-Ti-C-Ti layer and that below it. At each step we have performed a constrained relaxation keeping the z-coordinate of the middle Ti-atom of the exfoliated surface layer and the middle Ti-atom of the slab fixed. This step-wise detachment of the surface layer is done till the exfoliated layer does not interact with the rest of the slab.